Elevated Temperature Mechanical Performance of Historical Niobium Alloys

Eric Brizes [a]

Justin Milner [a]

[a] NASA Glenn Research Center, Cleveland, OH

TMS 2025. Las Vegas, NV. March 24

Introduction

- Niobium's unique combination of high melting point, low density, and excellent strength make it a prime candidate for re-entry vehicles and other high-temperature applications. The development of niobium (Nb) alloys was closely tied to the aerospace and defense advancements of the mid-20th century.

- **Historical Context**
  - In the 1960s, *Boeing* and *Wah Chang Corp*. initiated a cooperative effort to explore Nb-based alloys for re-entry shielding leading to the development of **C103** (*Nb-10Hf-1Ti, wt%*). [1]
  - The early 1970s saw intense Nb alloy research driven by the space race and missile defense needs. During this time, **FS85** (*Nb-28Ta-10W-1Zr*) was developed by *Fansteel*. [1]
  - Meanwhile, **Cb752** (*Nb-10W-2.5Zr*) was explored for elevated temperature structural aerospace components, yet no significant applications materialized. [1]
  - Later, in the mid-to-late 1970s, *Wah Chang* introduced **WC3009** (*Nb-30Hf-9W-1Zr*) as an oxidation-resistant alloy, though it ultimately failed to gain widespread adoption. [1]

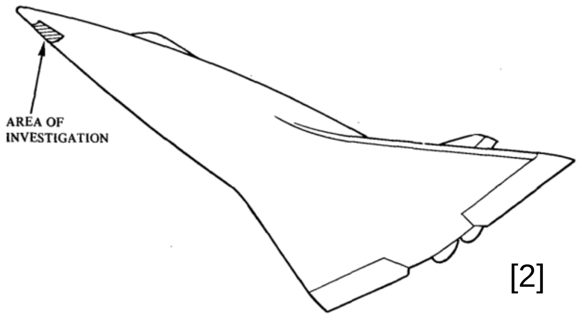

[2]

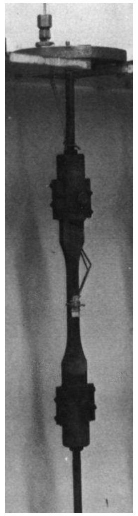

Motivation

- Refractory alloys, particularly Nb-based alloys, are experiencing a resurgence due to advancements in powder-based additive manufacturing.
- Researchers at NASA Glenn Research Center and Marshall Space Flight Center are actively evaluating a wide range of historical Nb alloys to identify candidates for modern aerospace applications.
- This study focuses on the performance of **C103**, **FS85**, **Cb752** and **WC3009**, assessing their mechanical properties at elevated temperatures when fabricated using Laser Powder Bed Fusion (L-PBF) additive manufacturing.
- The goal is to determine whether any of these legacy alloys retain potential for future aerospace use, especially in high-temperature environments requiring exceptional strength and creep resistance. Additionally, this property screening serves as a foundation for the development of next-generation Nb alloys.

(a)

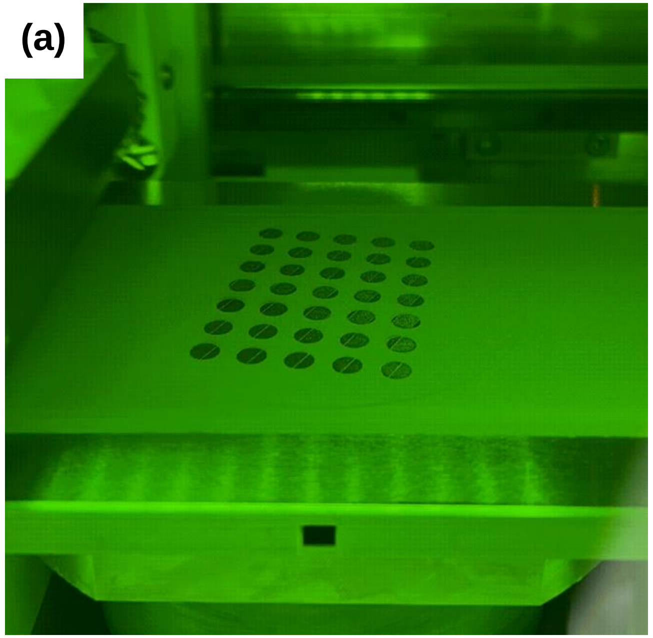

(b)

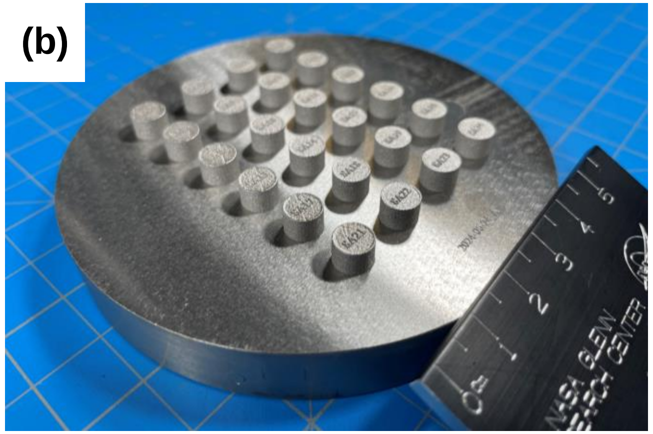

Nb alloy (a) L-PBF processing and (b) completed parameter development build

Outline

1. **Materials and Processing**
   - L-PBF Consolidation
   - Chemical Analysis
2. **Mechanical Testing**
   - Testing Equipment
   - Elevated Temperature Tension
   - Elevated Temperature Constant Load (Pseudo-Creep)
3. **Comparative Evaluation**
   - Microstructural Thermal Stability
4. **Conclusions**

Powder Materials

- **C103** *(Nb-10Hf-1Ti)*
  - D_{10} = 16.3 µm
  - D_{90} = 51.5 µm
- **Cb752** *(Nb-10W-2.5Zr)*
  - D_{10} = 13.2 µm
  - D_{90} = 66.2 µm ↑
- **FS85** *(Nb-28Ta-10W-1Zr)*
  - D_{10} = 16.4 µm
  - D_{90} = 46.8 µm
- **WC3009** *(Nb-30Hf-9W-1Zr)*
  - D_{10} = 30.7 µm ↑
  - D_{90} = 70.7 µm ↑

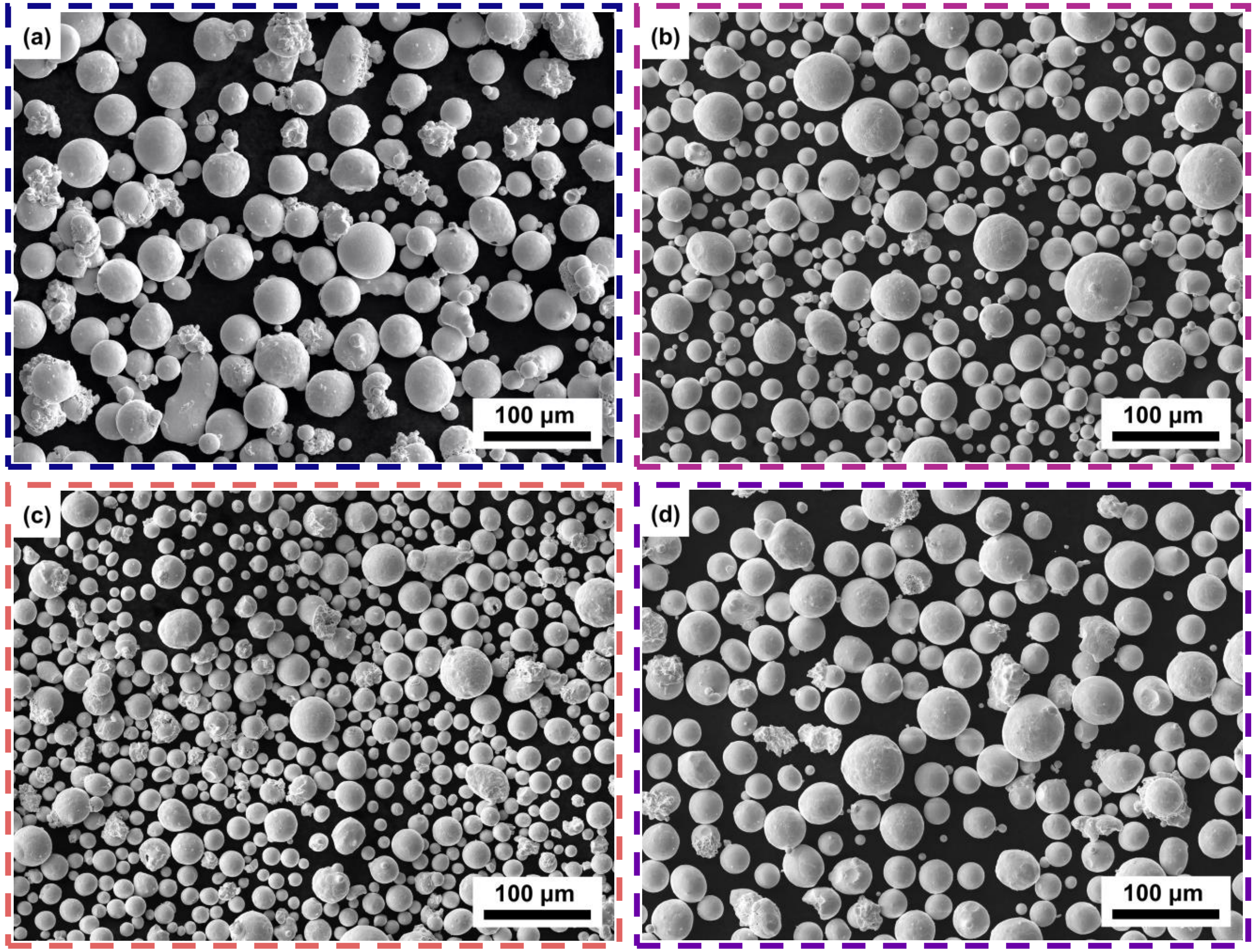

Secondary electron SEM micrographs of the (a) **C103**, (b) **Cb752**, (c) **FS85**, and (d) **WC3009** Nb alloy spherical powders

Laser Powder Bed Fusion

- *EOS M100*, Nb build plate, Argon atmosphere (<10 ppm O_2), 31.5 x 10 x 1.5 mm bowties

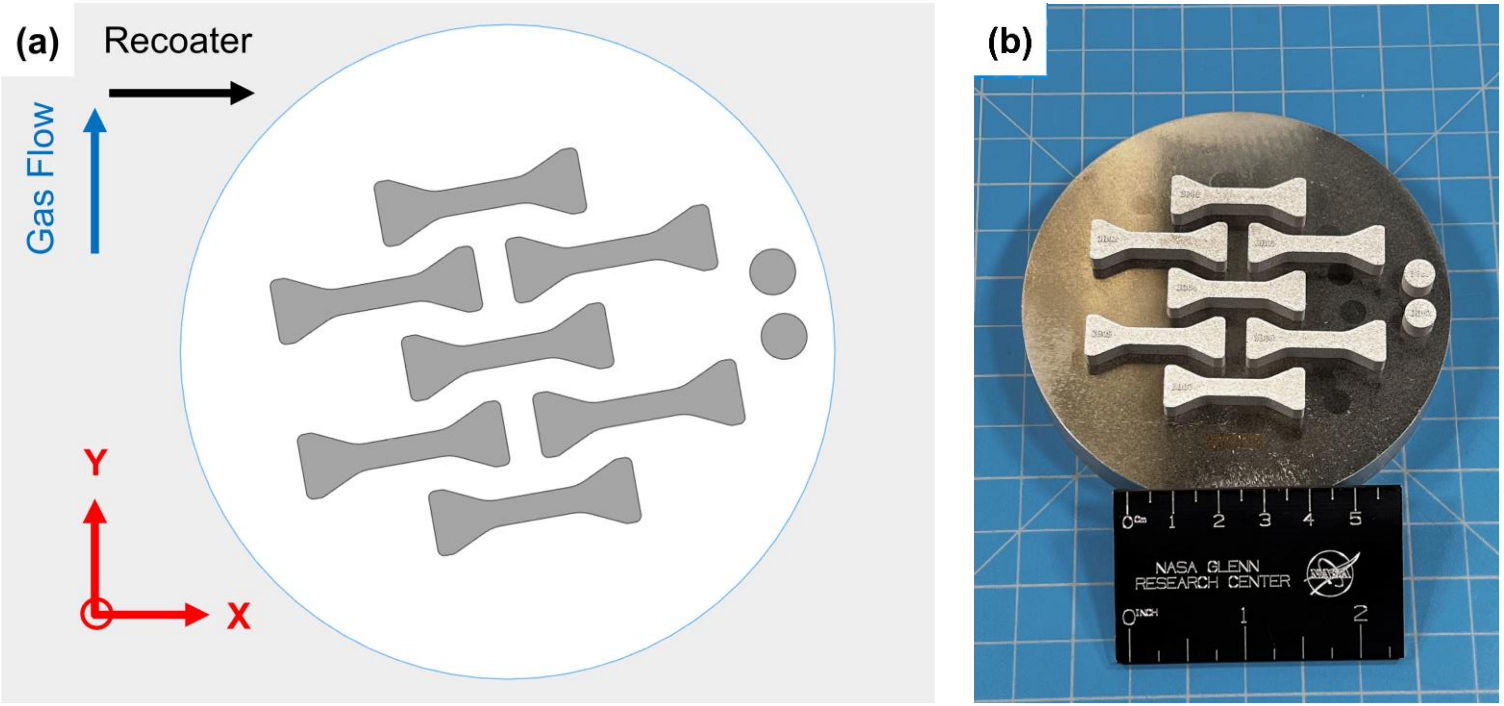

(a) Schematic L-PBF build layout and (b) image of the completed **C103** build

L-PBF volumetric energy density (VED) and material density measurements

Material	C103	Cb752	FS85	WC-3009
VED [J/mm^3]	115	140	120	120
Arch. Density [g/cc]	8.80	9.00	10.60	10.30
Optical Density [%]	99.92	99.89	99.96	99.89

Chemical Composition

- Determined via SEM-EDS and LECO Combustion analysis

Material	Nb [wt%]	W [wt%]	Hf [wt%]	Ta [wt%]	Ti [wt%]	Zr [wt%]	O [ppm]	N [ppm]	C [ppm]
L-PBF **C103** *(Nb-10Hf-1Ti)*	Bal.	0.27	9.85	0.36	0.92	-	425 ↑	58	19
L-PBF **Cb752** *(Nb-10W-2.5Zr)*	Bal.	9.93	-	-	-	2.82 ↑	376 ↑	102	15
L-PBF **FS85** *(Nb-28Ta-10W-1Zr)*	Bal.	10.05	-	27.71	-	0.16 ↓	524 ↑	115	7
L-PBF **WC3009** *(Nb-30Hf-9W-1Zr)*	Bal.	9.39	29.53	-	-	0.45 ↓	242	58	32

A dash symbolizes a result of “not measured/detected”

Elevated Temperature Mechanical Testing Equipment

- *Instron* Electro-Thermal Mechanical Testing (ETMT)
- Direct resistance heating (non-uniform thermal gradient)
- High-vacuum: < 10^{-5} Pa (< 10^{-7} Torr)
- Supports uniaxial tension & constant load (pseudo-creep)

1500 °C Test Thermal Profile

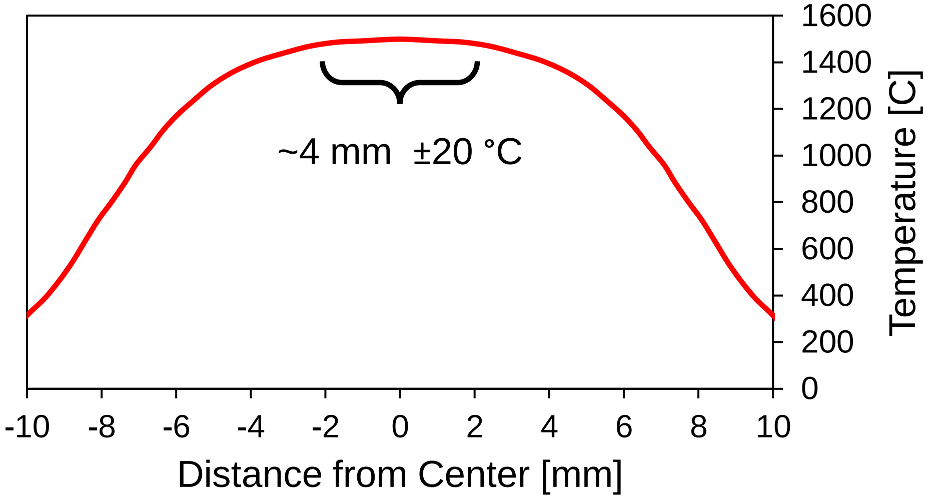

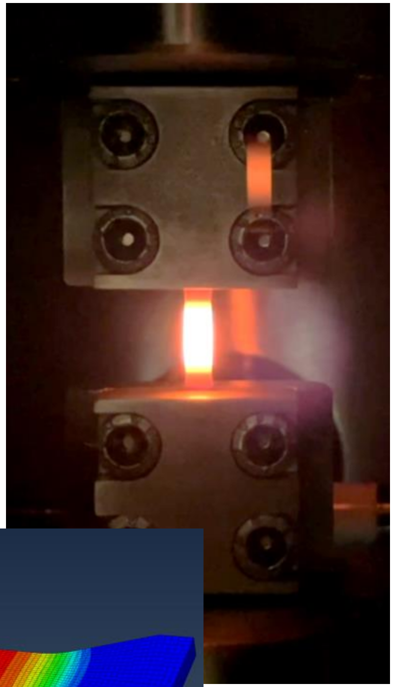

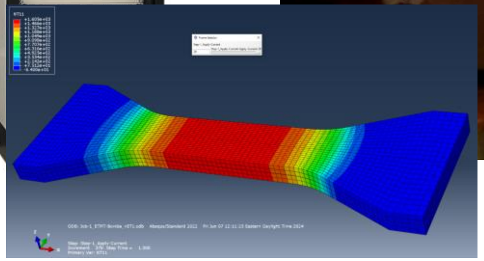

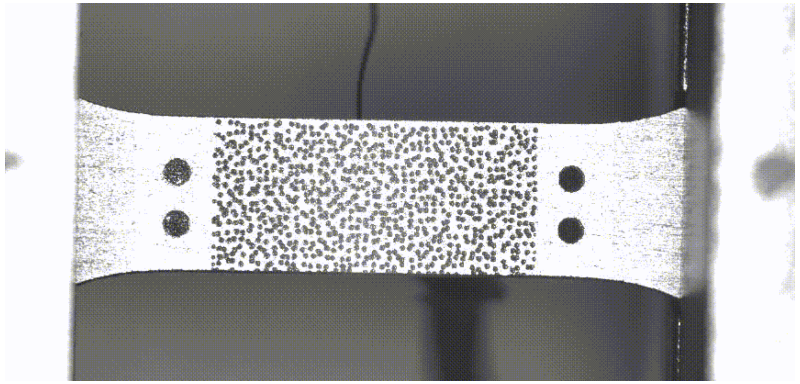

Elevated Temperature Uniaxial Tensile Testing

- At temperatures > 1300 ° C: **FS85** ≈ **Cb752** > **WC3009** > **C103**

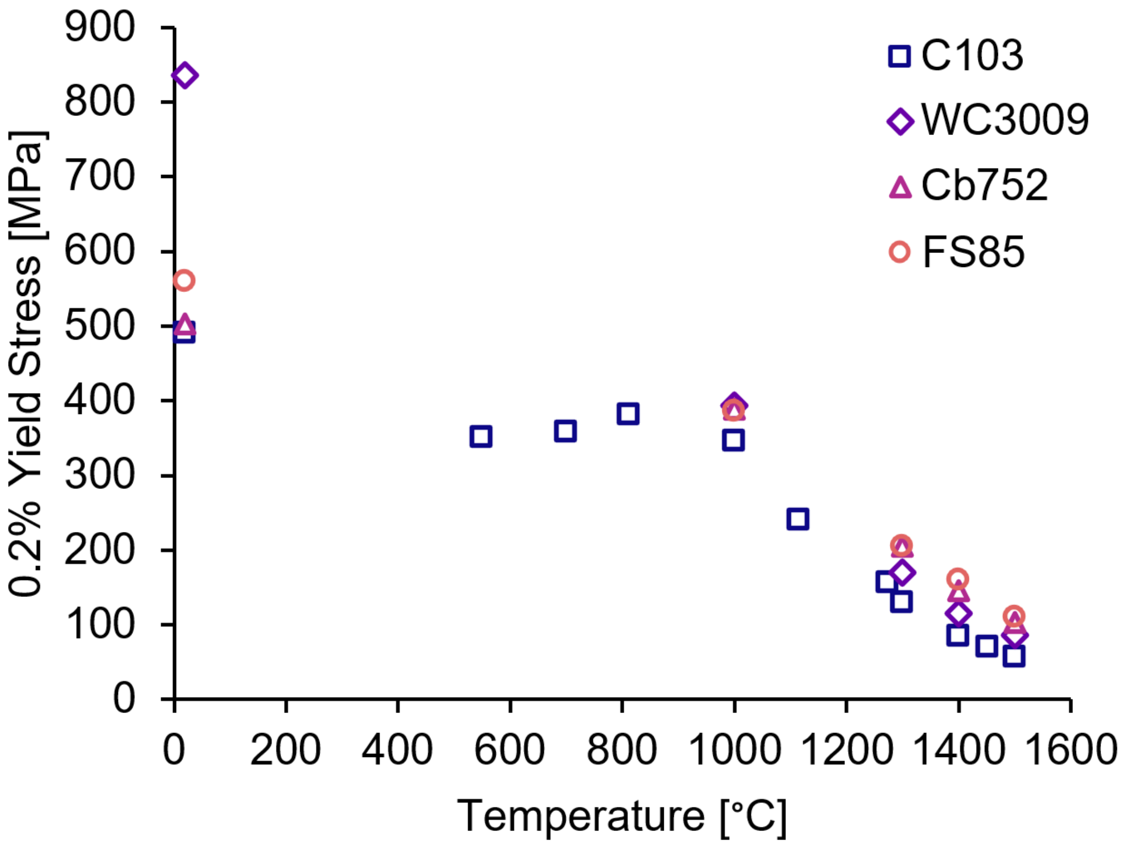

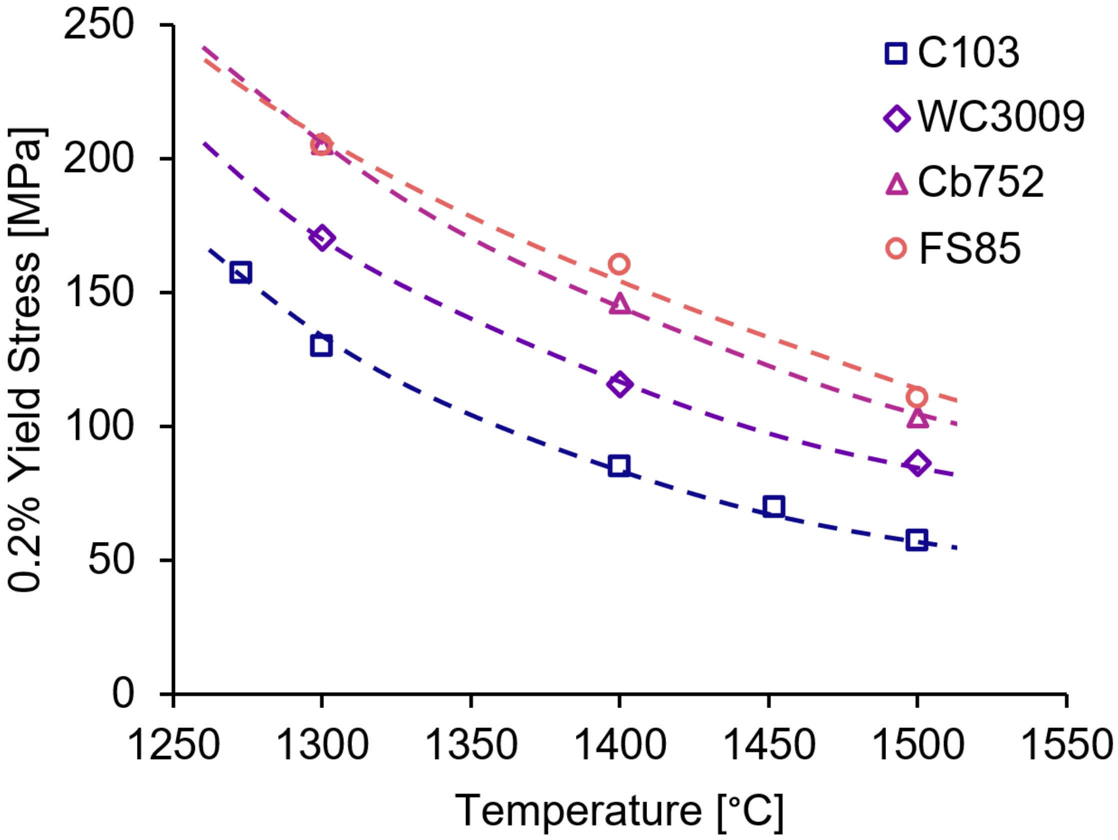

Note: 25 °C data for WC3009, Cb752, and FS85 were stress relieved at 1200 °C for 1 hour. All other data generated from samples stress relieved at 900 °C for 1 hour.

Elevated Temperature Constant Load (Pseudo-creep)

- At 1300 °C and a constant load of 50 MPa: **FS85** > **Cb752** > **WC3009** > **C103**

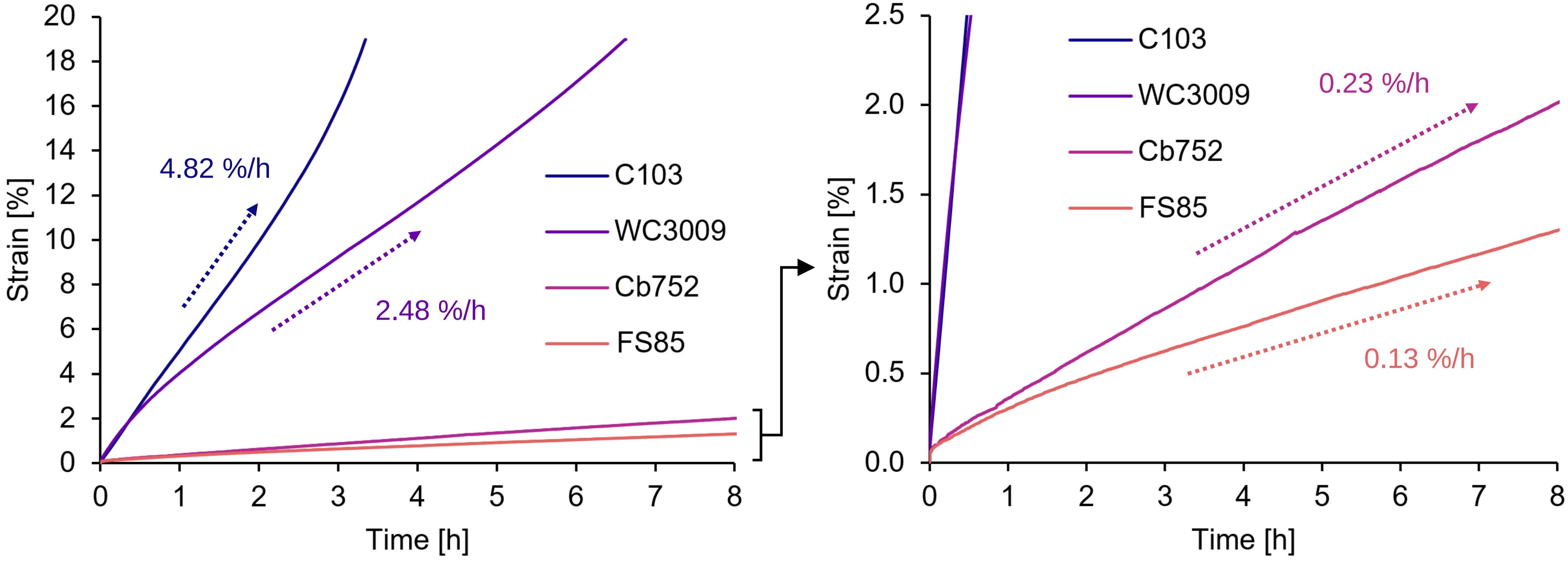

Microstructural Characterization: *L-PBF > SR > Tension*

- **C103** *1500 °C*

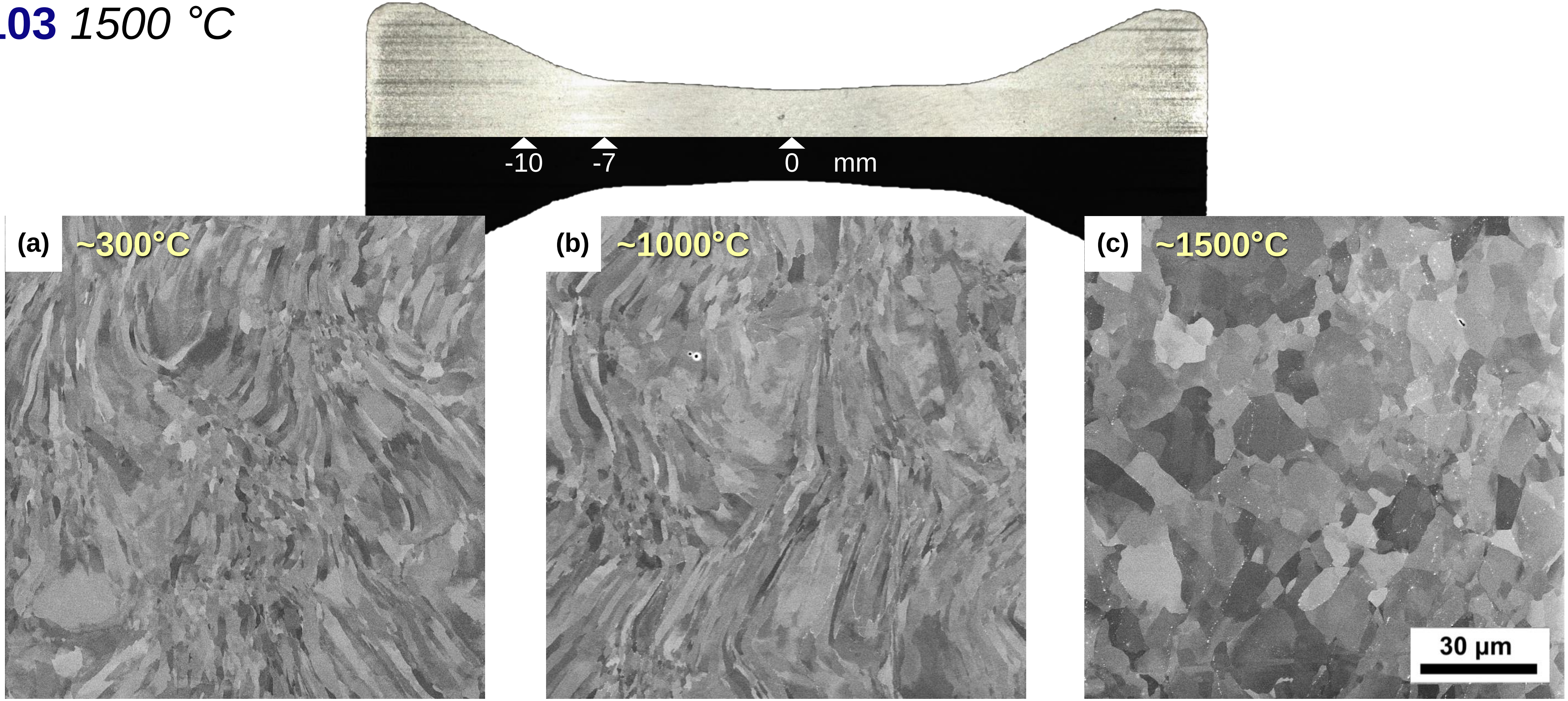

Low magnification secondary electron micrographs of the 1500 °C elevated temperature L-PBF **C103** at (a) -10, (b) -7, and (c) 0 mm from central axis

Microstructural Characterization: *L-PBF > SR > Tested*

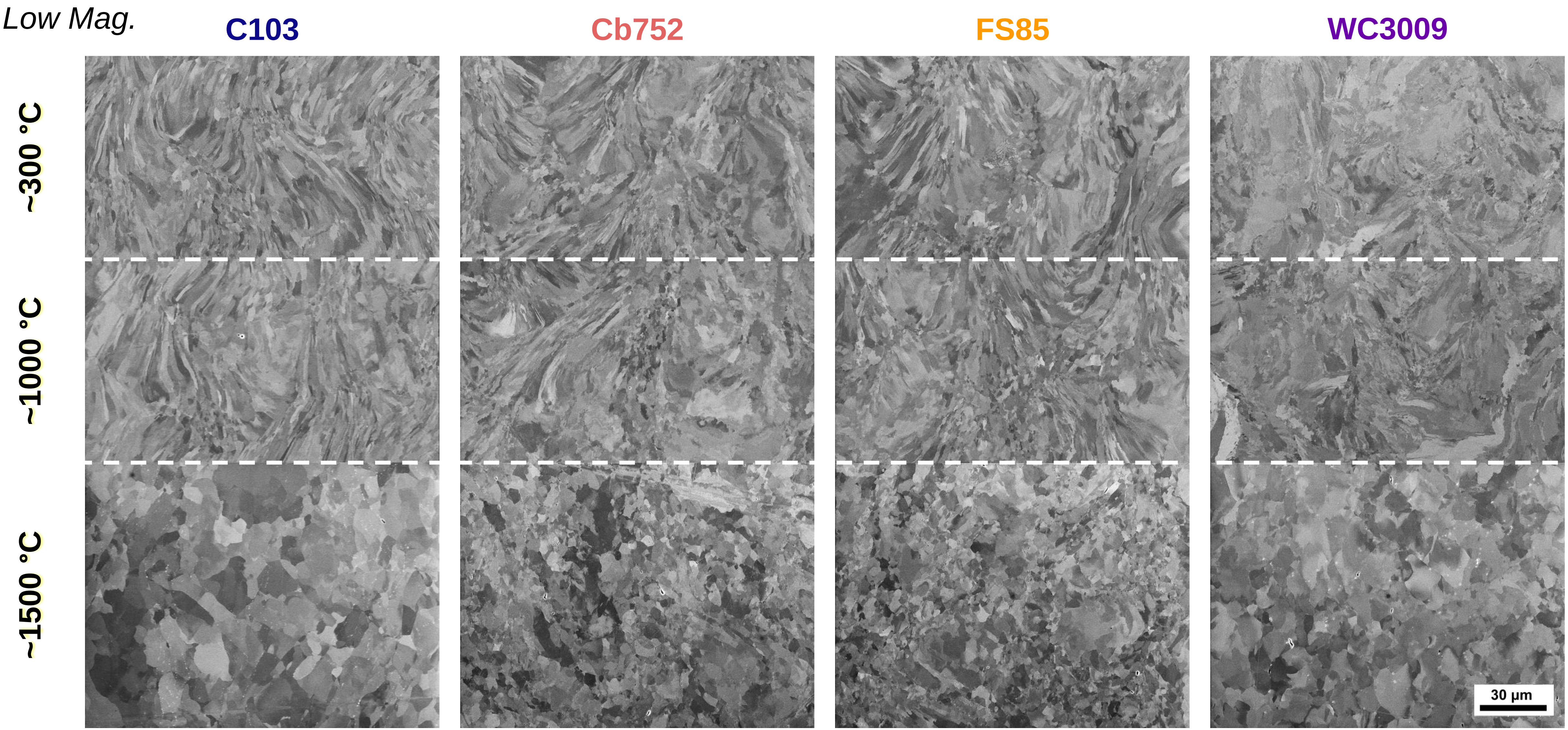

Microstructural Characterization: *L-PBF > SR > Tested*

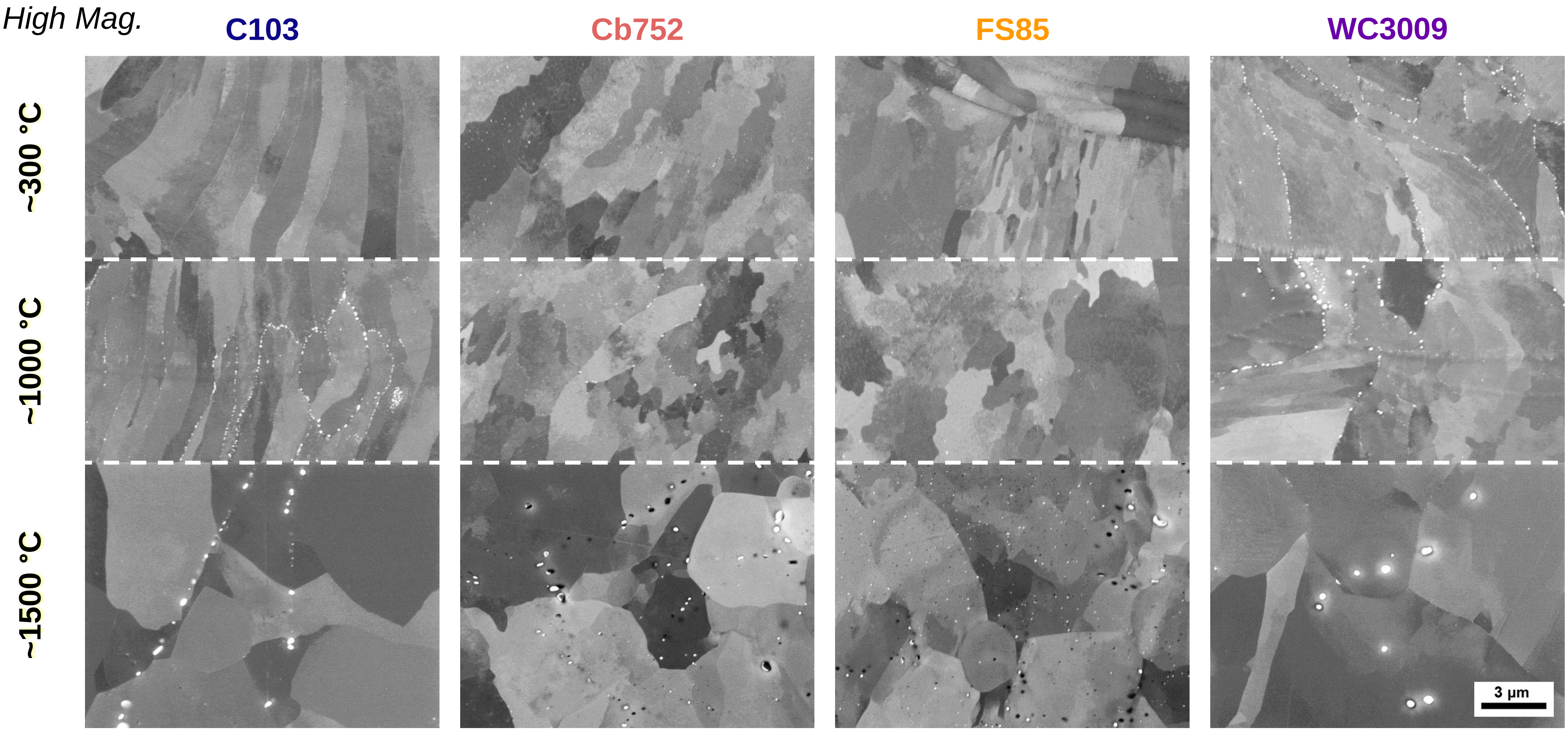

Microstructural Characterization: *L-PBF > SR > Tested*

High Mag.

~1500 °C

C103

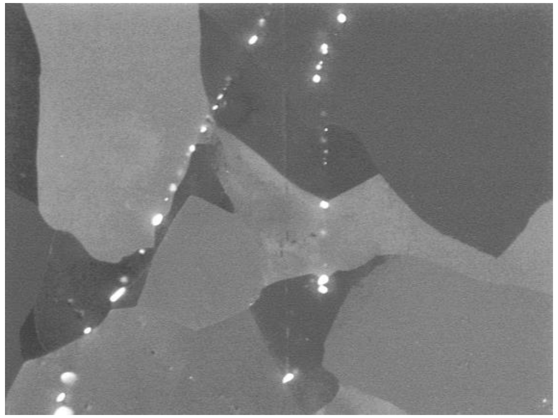

- Larger Grains
- Coarse HfO_2 not along GBs

5.34 at% **Hf**
0.24 at% O
~0.12 mol% HfO_2
5.22 at% excess Hf

Cb752

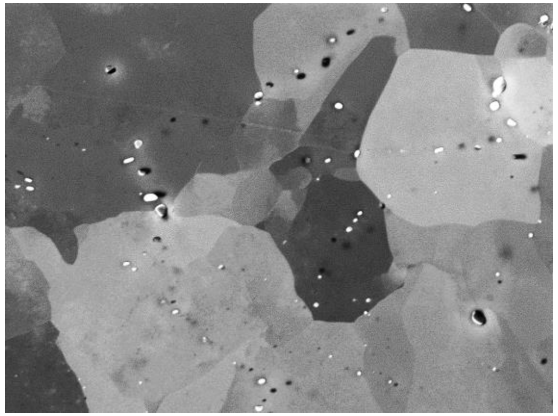

- Smaller Grains
- Coarse ZrO_2 occasionally along GBs

3.01 at% **Zr**
0.24 at% O
~0.12 mol% ZrO_2
2.89 at% excess Zr

FS85

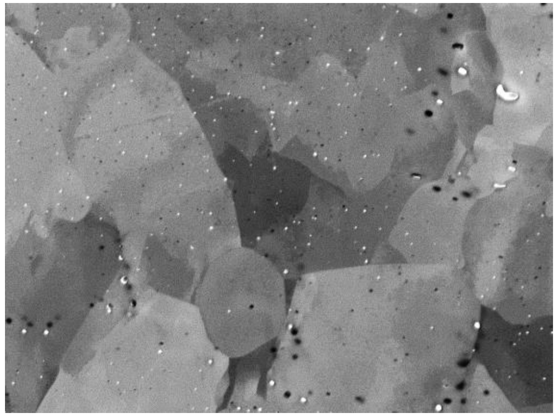

- Smaller Grains
- Coarse ZrO_2 along GBs, fine ZrO_2 intragranular

0.20 at% **Zr**
0.35 at% O
~0.17 mol% ZrO_2
0.03 at% excess Zr

**Near 1:2 Zr:O ratio (ideal stoichiometry)*

WC3009

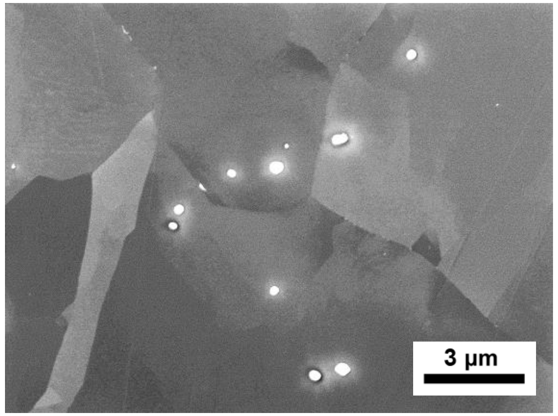

- Larger Grains
- Coarse HfO_2 not along GBs

18.91 at% **Hf**
0.14 at% O
~0.07 mol% HfO_2
18.84 at% excess Hf

Conclusions

1. The L-PBF process successfully consolidated all examined historical niobium alloys with all relative densities ≥ 99.89% (determined by optical microscopy and image analysis).
2. Elevated temperature uniaxial tensile testing determined the ranking of each L-PBF consolidated historical niobium alloy in terms of yield and ultimate tensile strength at temperatures greater than 1300 °C: **FS85** ≈ **Cb752** > **WC3009** > **C103**.
3. 1300 °C pseudo-creep testing performed at a constant load of 50 MPa determined the ranking of each L-PBF consolidated historical niobium alloy in terms of steady-state creep rate: **FS85** > **Cb752** > **WC3009** > **C103**.
4. Examination of the 1500 °C tensile specimen microstructure of each historical niobium alloy showed:
   - The high Hf-containing alloys (**C103** and **WC3009**) exhibited significant HfO_2 precipitate coarsening, and the precipitates were ineffective at pinning grain boundaries.
   - The Zr-containing alloys (**Cb752** and **FS85**) exhibited ZrO_2 precipitate coarsening; however, the precipitates formed a finer dispersion (particularly when the Zr:O atomic ratio was near stoichiometric (1:2).

References

1. J. Hebda, "Niobium Alloys and High Temperature Applications," Wah Chang - An Allegheny Technologies Company, Albany, 2001.
2. W.E. Black et al., "Evaluation of Coated Columbium Alloy Heat Shields for Space Shuttle Thermal Protection System Application," *NASA CR-112119*, 1972.